EARTH SURFACE PROCESSES AND LANDFORMS
Earth Surf. Process. Landforms **38**, 655–660 (2013)

Published online 8 March 2013 in Wiley Online Library
(wileyonlinelibrary.com) DOI: 10.1002/esp.3392

Letters to ESEX

The effect of tide on the hydrology and morphology of a freshwater river

Scott H. Ensign,[1,3]* Martin W. Doyle[2] and Michael F. Piehler[3]
[1] Curriculum for the Environment and Ecology, University of North Carolina at Chapel Hill, Chapel Hill, NC, USA
[2] Department of Geography, University of North Carolina at Chapel Hill, Chapel Hill, NC, USA
[3] Institute of Marine Sciences, University of North Carolina at Chapel Hill, Morehead City, NC, USA

Received 30 July 2012; Revised 9 January 2013; Accepted 17 January 2013

*Correspondence to: Scott H. Ensign, Aquatic Analysis and Consulting, LLC, Morehead City, NC USA. E-mail: scott@aquaco.us

ESPL
Earth Surface Processes and Landforms

ABSTRACT: How does river hydrology and morphology change due to tidal influence? We contend that this is a question of particular consequence to many earth surface disciplines, but one that has not been adequately addressed. Previous studies have relied on gradients in channel morphology and stratigraphy to infer energy regime of channels. However, in tidal rivers geomorphology influences the energy regime while the energy regime influences morphology; thus, geomorphic and stratigraphic patterns do not fully resolve the mechanisms which lead to change. We addressed this problem by comparing measurements of hydraulic energy and channel morphology along a tidal gradient to predictions of these characteristics in the absence of tides, and attributed the differences to tidal processes. Measurements of discharge, channel area, and energy dissipation (in kJ day^{-1}) were made over a 24·8 hour period at four sites spanning the non-tidal to tidal freshwater Newport River, NC. We then predicted those characteristics under non-tidal conditions using hydraulic geometry relationships and literature values from coastal plain rivers. Discharge was enhanced more than 10-fold by tide, and this tidal effect increased from upstream to downstream along the tidal gradient. Cross-sectional area increased three-fold due to tide. Energy dissipation measured in the upper tidal river was four-fold lower than predicted to occur in the absence of tide because tides decreased average velocity and discharge. Energy dissipation measured downstream was similar to that predicted to occur without tides, although there was large uncertainty in predicted values downstream. While this limited dataset does not permit us to make broad generalizations for definitive models, it does provide a proof-of-concept for a new approach to addressing a critical problem at the interface of fluvial and coastal morphology. Copyright © 2013 John Wiley & Sons, Ltd.

KEYWORDS: tidal river hydrology; geomorphology; sea level rise; hydraulic geometry; tidal freshwater river

Introduction

In low gradient, alluvial coastal plain rivers, tides extend far upstream beyond the limit of saltwater influence, creating vast stretches where river flow reverses and where channel and floodplain water depth fluctuate continually. How does a river channel's hydrology and morphology change as it is progressively exposed to estuarine tides as sea level rises? These changes are of consequence to many disciplines. To geologists, tidal rivers represent a cross-over between fluvial and estuarine process-dominance, where the relative influence of fluvial versus estuarine processes are unclear. For biogeochemists and ecologists, tidal rivers are a critical zone affecting the transport of carbon and other biologically-relevant elements from watersheds to estuaries. Despite study from a variety of perspectives and growing documentation of the patterns in tidal river morphology, the mechanisms by which tides affect these patterns are not fully understood (Ensign *et al.*, 2012). In this letter we argue that new approaches are needed to investigate the mechanisms by which tides alter river morphology.

Geomorphic patterns have been used to investigate how rivers change due to tides. For example, the downstream increases in channel width and cross-sectional area have been used to infer a chronology of channel adjustment (Langbein, 1963; Davies and Woodroffe, 2010). Gardner and Bohn (1980) suggested that increased width was a geomorphic response of the river channel forced to accommodate higher discharge and tidal energy, while Wright *et al.* (1973) suggested that these longitudinal trends were influenced by the degree to which the tidal wave approximated a standing versus progressive wave. Other spatial patterns, such as channel planform and sinuosity, have been suggested to relate to the region where fluvial and estuarine sediment loads converge, which is in turn believed to be a function of the tidal-versus-fluvial energy regime of the channel (Dalrymple and Choi, 2007).

In addition to the relationships between geomorphic pattern and tidal influence, stratigraphy of sediments along the tidal–fluvial transition follow predictable patterns in sequences related to the changing energy regime of the channel. These techniques and facies models are reviewed by Dalrymple and Choi (2007), and other researchers have focused specifically

on identifying the transition from fluvial to tidal freshwater (Woodroffe *et al.*, 1989; Pizzuto and Rogers, 1992). The stratigraphic approach to studying tidal influence on river channel morphology uses sediment characteristics, bedforms, and biological evidence to infer the hydrologic regime of the channel during periods of sea level rise. Hydrologic characteristics such as bi-directional flow and the magnitude of flow can be detected in stratigraphic records, as well as the spatial patterns in channel morphology.

Energy regime is often used in the explanation of riverine adjustment to tidal flow. Unlike in rivers, in tidal environments energy can be both a dependent and independent variable (Langbein, 1963). Feedbacks between tides and river morphology subsequently change the tidal dynamics within the channel, and therefore the spatial gradient in energy dissipation is the result of a morphodynamic feedback between morphology and tidal hydrology (Wright *et al.*, 1973; Friedrichs, 1995). Because of these feedbacks between channel hydrology and geomorphology, contemporary geomorphic and stratigraphic patterns cannot necessarily be interpreted as a result of a particular energy regime, since the energy regime itself is dependent on channel morphology. To understand the extent to which the energy regime of rivers changes with tidal influence and the underlying processes, tidal energy regime must be related with the energy regime that would exist in the absence of tides.

A technique is needed that allows determination of the difference between river hydrology and morphology before and after tidal influence at a single location. One approach is to predict what the fluvial characteristics would be without tidal influence and compare these to contemporary observations, the difference being attributable to tidal influence. The fluvial characteristics fundamental to describing tidal influence in rivers are discharge, channel cross-section area, and hydraulic energy, the latter being the most important. Energy dissipation (in J m^{-1}) is a common metric in fluvial research (e.g. Molnár and Ramírez, 1998), estuarine research (e.g. van der Wegen *et al.*, 2008), and stratigraphic models (Dalrymple and Choi, 2007) because it couples the force of moving water with the potential for geomorphic work. The energy contributed by tides is predicted to affect river morphology and sediment transport over time (Dalrymple and Choi, 2007), and some studies have quantified patterns in energy along a river's tidal gradient (Chen *et al.*, 2005). However, it remains unknown how energy dissipation at a location, and subsequently the potential for geomorphic work, change as sea level introduces tide into previously non-tidal rivers.

We addressed this challenge by making a series of observations of discharge, channel cross-section, and energy dissipation in a tidal river and then predicting what these characteristics would be in the absence of tide. Our goal was not to provide definitive answers to the question of how tides alter rivers, but rather to develop a new approach that allows insight into this important question.

Methods

Study area

The Newport River drains a 310 km^2 watershed in North Carolina, USA. Three sites along the tidal freshwater river were located 2·3 km ('upstream'), 5 km ('midstream'), and 9 km ('downstream') from the head-of-tide, respectively, and one site ('Atidal') was above tidal influence. The river is a meandering, single channel with cut banks and depositional bars only found between the Atidal and upstream sites.

Morphology, discharge, and stream power

Discharge and morphology at the Atidal site was measured in June 2007 and February 2009. A Sontek Flowtracker acoustic Doppler velocimeter (SonTek/YSI, San Diego, CA) was used to measure velocity at 0·6 × depth at 0·5 m intervals across the channel (standard deviation of 0·016 m s^{-1}), and discharge was calculated as the summed product of depth and velocity. Bankfull cross-section area at all sites was determined using the bench index method of Riley (1972).

Observations of discharge (Q) were made at the upstream, midstream, and downstream sites over two semi-diurnal tidal cycles (24·8 hr, hereafter referred to as a tidal day) once in June 2008 and once in February 2009. River discharge was calculated from current velocities measured at one minute intervals using a horizontally-mounted Nortek 2 mHz Aquadopp (NortekUSA, Annapolis, MD) current profiler. Velocity was measured across a 10 m channel width at 1 m intervals (standard deviation of 0·022 m s^{-1}). Depth was measured at 1 m intervals across the channel, and water level change was recorded every minute using Intech TruTrak (Intech Instruments Ltd, Christchurch, New Zealand) capacitance rods (accuracy ± 15 mm). Depth-averaged velocity and random error in velocity for the measured and extrapolated portion of the channel was determined using the methods in Simpson and Bland (2000).

Current profiler data were not always reliable because of signal interference from the channel bottom, and measurements whose range in signal-to-noise ratio included background levels were discarded. This was a problem at the midstream site, so additional synoptic surveys of velocity were made at these sites during ebb and flood tide using a Sontek Flowtracker. The cross-channel ratios of velocity from synoptic surveys were used to extrapolate the profiler data to the limited portions of the channel where signal-to-noise ratios were unreliable.

Stream power '... refers to the time rate of potential energy expenditure (i.e. conversion of potential energy to kinetic energy that is dissipated in overcoming internal and boundary friction, in transporting sediment and in eroding the channel perimeter) as water travels downslope in a channel' (Rhoads, 1987). Energy dissipation is equivalent to the integration of stream power over time. We calculated cross-sectional stream power (in kg m s^{-3}) as:

$$\Omega = \rho g S Q \tag{1}$$

where ρ is the density of water, g is gravitational acceleration, S is the energy grade slope (hereafter called energy slope), and Q is discharge (Rhoads, 1987). At the Atidal site, energy slope was calculated using a standard formulation for steady flow:

$$S = \left(\frac{U \times n}{R_h^{2/3}}\right)^2 \tag{2}$$

where U is the average velocity, n is the Manning's friction term, and R_h is the hydraulic radius. A Manning's n of 0·06 ± 0·01 was used, representing the mean and standard deviation from 12 coastal plain, non-tidal streams in North Carolina [Geratz, personal communication August 2010, see Sweet and Geratz (2003) for further details; sinuosity of the streams (1·2–1·5) was primarily responsible for elevating the reach-scale estimate of Manning's n]. For both the Atidal and tidal sites, stream power was integrated over 24·8 hour to calculate the energy dissipation which was expressed on the basis of a 1 m length of stream channel (in kg m^2 s^{-2}).

Energy slope at the tidal sites (and subsequently stream power) were calculated using the formula for unsteady flow:

$$S = -\left\{\frac{\partial \eta}{\partial x} + \frac{U}{g}\frac{\partial U}{\partial x} + \frac{1}{g}\frac{\partial U}{\partial t} + \frac{(h+\eta)}{2\rho}\frac{\partial \rho}{\partial x}\right\} \quad (3)$$

where η is water level, x is distance, h is depth (Knight, 1981). The first term in Equation 3, the water surface slope, was measured between the upstream to downstream sites (6730 m reach length) using elevation benchmarks established with a Trimble TSC2 RTK GPS (Trimble Navigation Limited, Sunnyvale, CA) combined with water level measurements. The uncertainty in water surface slope measurements due to water level and elevation measurement error was $4{\cdot}0 \times 10^{-6}$.

Convective acceleration, the second term in Equation 3, was calculated at one minute intervals with dU/dx assumed to be a separate constant during flood and ebb tide. These constants were calculated from the difference in mean velocity observed during a tide stage between adjoining sites in the direction of flow. At the upstream site we assumed that velocity decreased to zero 1 km up-river during flood tide based on personal observation. At the downstream site, velocity was assumed to decrease 4% between the downstream site and the end of the fluvial channel 6 km downstream (Mohammad, 1961). Local acceleration, the third term in Equation 3, was calculated from velocity data averaged over a five minute period. During the study period there was no saltwater intrusion into the river, therefore density gradients were not considered and the final term of Equation 3 was dropped. The second and third terms have been found to be relatively small compared to the first term in tidal channels (Knight, 1981; Buschman *et al.*, 2009), and thus the uncertainty associated with the assumptions for terms two and three should have little influence on S. Total relative random error in stream power was calculated from the random error in Q and S.

Predicted non-tidal morphology, discharge, and stream power

The predicted bankfull channel cross-sectional area (A_{bkf}, in m^2) for each site in the absence of tidal flow was estimated as $9{\cdot}43 \times k \times A_w^{0.74}$, where A_w is watershed area (in m^2), and k is a conversion constant between ft^2 and m^2 ($r^2 = 0{\cdot}96$, Sweet and Geratz, 2003). Predicted cross-sectional area at the time of the study was calculated by multiplying the ratio channel area:A_{bkf} at the Atidal site by the A_{bkf} predicted for the upstream, midstream, and downstream sites. Average values of R_h and Manning's n from non-tidal coastal plain streams in North Carolina (Sweet and Geratz, 2003) were assumed to apply to the Newport River in the absence of tides. Water yield (in m^3 km^{-2} s^{-1}) at the Atidal site was multiplied by the watershed area of the other sites to predict discharge in the absence of tides. The stream power and energy dissipation expected to occur in the absence of tidal influence at the upstream, midstream, and downstream sites was determined using Equation 1, but with predicted values assuming no tides rather than observed morphology and discharge.

Results

Observed versus predicted morphology and discharge

Observed channel depth, width, and R_h generally increased from the Atidal site to the downstream site (Table I). Tidal variation in depth was greatest at the midstream site in 2009 (0·8 to 1·6 m) while variation in width was greatest at the downstream site in 2008 (20 to 27 m). Velocity was higher at the Atidal site than the upstream tidal site, although maximum velocities at the midstream and downstream sites were greater than the Atidal site. Maximum salinity of 0·56 occurred downstream. Effluent from a wastewater treatment plant adjacent to the midstream site likely affected salinity values.

Observed bankfull channel cross-sectional area at the Atidal, upstream, midstream, and downstream sites was 19 m^2, 15 m^2, 47 m^2, and 64 m^2, respectively, while predicted values for these sites in the absence of tide were 12 m^2, 13 m^2, 15 m^2, and 19 m^2. The R_h value was predicted to be 1·35 m (± 0·47 m standard deviation) based on literature values for non-tidal coastal plain streams in North Carolina. The predicted R_h was higher than that observed at the Atidal site but was within the range of observed values at the tidal sites. Observed R_h increased from the Atidal site to the downstream site.

Observed discharge at the Atidal site was 0·606 m^3 s^{-1}. Observed discharge at all tidal sites showed an oscillating pattern indicative of tidal influence, with peak discharge occurring during ebb tide upstream and midstream, but during flood tide downstream (Figures 1–3). Predicted discharge was generally less than the observed values, with the difference between peak and predicted discharge increasing from upstream to downstream.

Observed versus predicted stream power and energy dissipation

Stream power increased along the tidal continuum, with peak values occurring during ebb tide upstream but during flood tide

Table I. Hydrologic and geomorphic characteristics of Newport River from June 3–10, 2008

Tide	Parameter	Atidal	Upstream	Midstream	Downstream
ebb	depth (m)	0·4	1·2 (1·0, 1·5)	1·1 (0·9, 1·6)	1·4 (1·2, 1·8)
	width (m)	6·0	6·8 (6·5, 7·0)	22 (18, 24)	22·7 (20·0, 27·0)
	velocity (m s^{-1})	0·25	0·10 (0, 0·18)	0·19 (0, 0·47)	0·29 (0, 0·41)
	R_h (m)	0·4	0·9 (0·8, 1·1)	1·1 (0·8, 1·4)	1·3 (1·1, 1·7)
	salinity	no data	0·05 (0·05, 0·07)	0·14 (0·07, 0·30)	0·12 (0·07, 0·56)
flood	depth (m)	—	1·3 (1·0, 1·5)	1·3 (0·9, 1·6)	1·7 (1·2, 1·8)
	width (m)	—	7·0 (6·5, 7·0)	23 (18, 24)	25·0 (21·0, 27·0)
	velocity (m s^{-1})[a]	—	−0·07 (0, –0·12)	−0·19 (0, –0·33)	−0·32 (0, –0·50)
	R_h (m)	—	1·0 (0·8, 1·1)	1·2 (0·8, 1·5)	1·6 (1·1, 1·8)
	salinity	—	0·05 (0·05, 0·05)	0·09 (0·02, 0·30)	0·15 (0·07, 0·56)

Note: Data presented as: mean (minimum, maximum). Channel depth, width, and velocity are the average of all cross-channel measurements.
[a]Negative velocity indicates upstream flow.

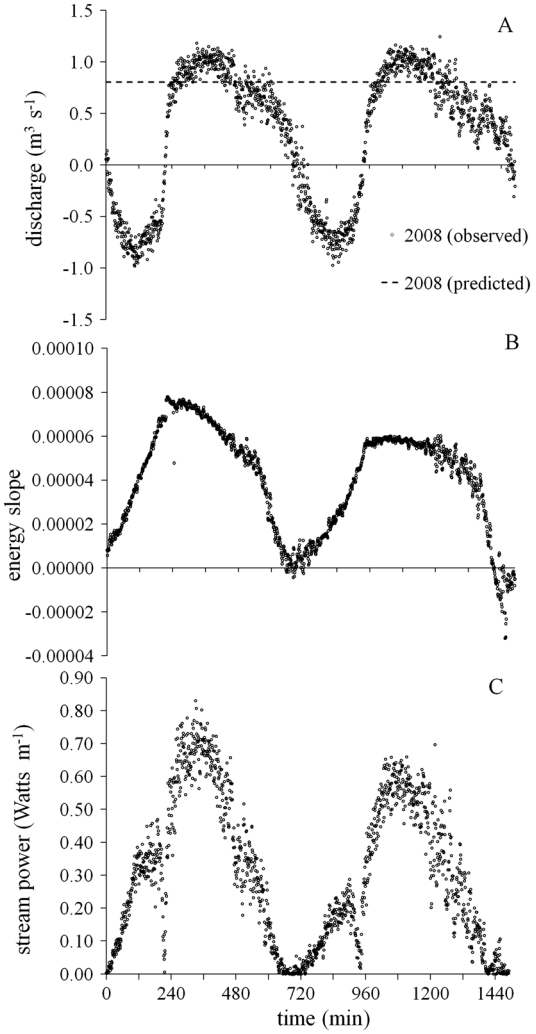

Figure 1. Upstream site tidal cycle measurements of discharge (A), energy slope (B), and stream power (C). Solid and dashed lines indicate the discharge predicted at the upstream site in the absence of tides; predicted energy slope was 0·00015 and predicted stream power was 1·15.

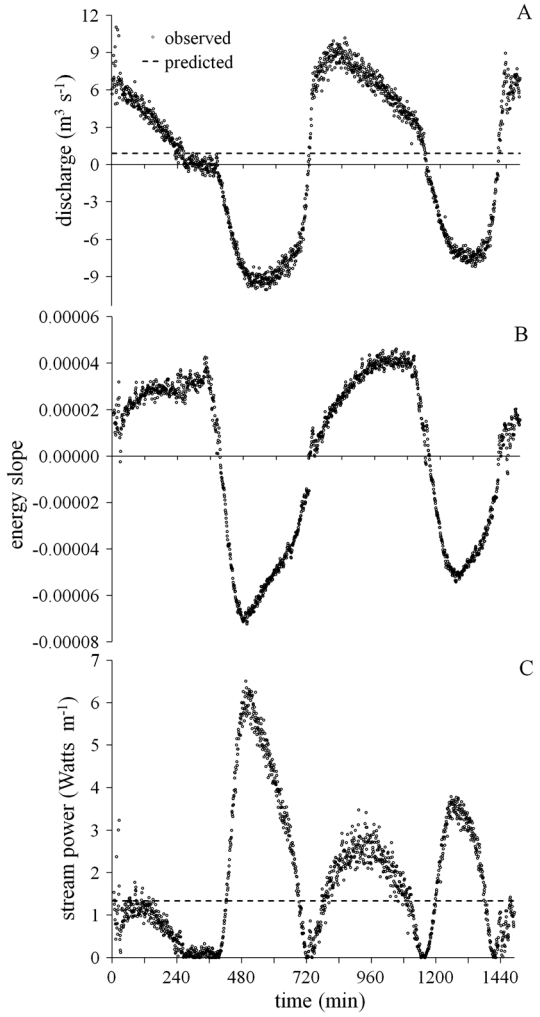

Figure 2. Midstream site tidal cycle measurements of discharge (A), energy slope (B), and stream power (C). Solid and dashed lines indicate the discharge predicted at the midstream site in the absence of tides; predicted energy slope was 0·00015.

downstream (Figures 1–3). Observed stream power was lower than predicted in the absence of tides upstream, but was within the same range as the non-tidal predictions midstream and downstream. Observed and predicted stream power midstream and downstream were similar because tidally-enhanced discharge over-compensated for the lower S than would occur in the absence of tides (Figures 1–3). The value of S displayed a similar sinusoidal trend as discharge over a semi-diurnal tidal cycle, but was lower than predicted would occur in the absence of tides at all sites (Figures 1–3).

Total energy dissipation (integration of stream power over time) averaged 11 kJ, 84 kJ, and 229 kJ per lunar day at the upstream, midstream, and downstream sites (Figure 4). These values were generally less than that which occurred at the Atidal site due to tidal fluctuations in Q and S. The observed energy dissipation at the upstream site during both years and the midstream site in 2009 was less than predicted in the absence of tidal influence, regardless of the assumptions made about non-tidal channel geomorphology and the random error in Q and S (Figure 4). At the midstream site in 2008 and the downstream site during both years the observed energy dissipation was similar to what was predicted to occur in the absence of tides. The large potential error in predicted energy dissipation downstream was due to the range in Manning's n and R_h used to account for uncertainty in these parameters.

Discussion

The primary objective of this study was to demonstrate a technique that would allow differentiation between tidal and fluvial discharge and energy dissipation. We found that discharge was enhanced more than 10-fold by tide, and that this tidal effect increased along a gradient of tidal influence. Stream power and energy dissipation were suppressed by tide at the upper extent of tidal influence (observed energy dissipation plus uncertainty estimate was less than predicted energy dissipation minus uncertainty estimate). The overall effect of tidal hydrology on channel morphology was a three-fold increase in bankfull channel cross-sectional area. Given the limited temporal extent of the energy dissipation measurements, the results are not intended to provide broadly applicable conclusions, but rather to provide a proof-of-concept of a new field-based approach to studying tidal rivers. The data illustrate important relationships between hydrology, morphology, and energy regime in tidal rivers from which hypotheses can be developed for further research.

Energy dissipation provides a metric for calculating the influence of tide on turbulence and sediment transport in rivers. The portion of this energy that is spent eroding, suspending, and transporting sediment within the river is fundamental to the morphology of the channel. By measuring Q, S, and the factors contributing to S (U, R_h), we were able to discern the hydrologic and morphologic influence of tides at the upstream

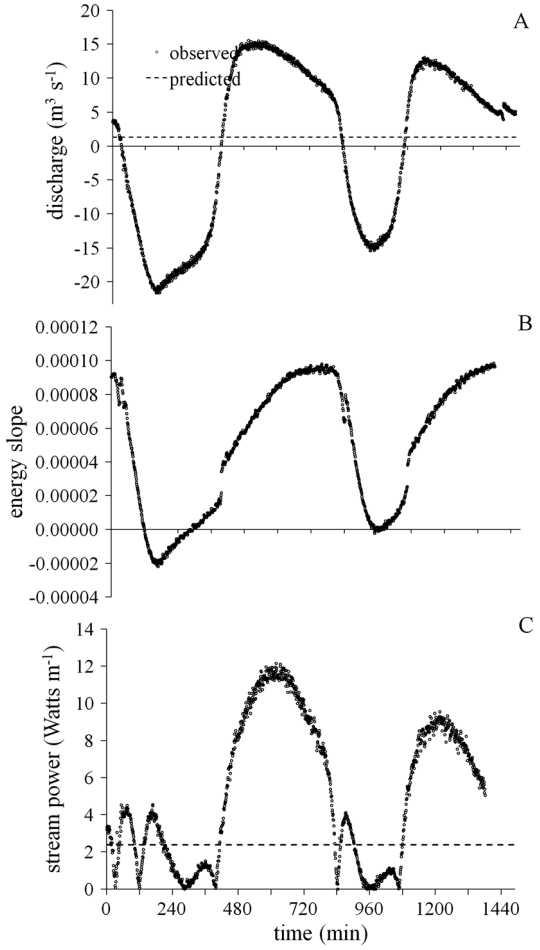

Figure 3. Downstream site tidal cycle measurements of discharge (A), energy slope (B), and stream power (C). Solid and dashed lines indicate the discharge predicted at the downstream site in the absence of tides; predicted energy slope was 0·00019.

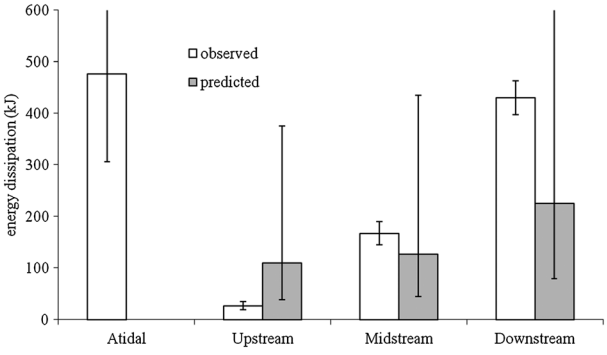

Figure 4. Observed and predicted energy dissipation (per lunar day per 1 m reach of river). Predicted values are those expected for each site in the absence of tides. Two combinations of A_{bkf}, R_h, and Manning's n were used to calculate a lower and upper bound for the predicted energy slope, which was subsequently used to calculated energy dissipation. A lower bound was calculated by combining a large channel area prediction (regression prediction + standard error), a high R_h (1·82, mean + one standard deviation), and a low Manning's n (0·05, mean – one standard deviation). An upper bound was calculated using a small channel area prediction (regression prediction – standard error), a low R_h (0·88, mean – one standard deviation), and a high Manning's n (0·07, mean + one standard deviation).

site. While peak Q increased relative to its predicted non-tidal condition along the length of the tidal Newport River (thereby increasing energy dissipation), S decreased along the tidal gradient (thereby decreasing energy dissipation) (Table I). Thus, tide had two countervailing effects on energy dissipation. At the upstream site, the reduction in S was proportionally greater than Q, and consequently energy dissipation was lower throughout the tidal cycle than would have occurred in the absence of tides. While we could not distinguish the tidal from predicted non-tidal energy dissipation at the midstream and downstream sites, the relative increase in peak Q was greater than the relative decrease in S.

Energy dissipation did not increase as a simple function of tidal amplitude and tidal water flow. Instead, tides affected channel morphology (R_h, depth, width) and Q such that there was a non-linear trend in energy dissipation along a tidal gradient. Non-linear patterns in energy dissipation along a tidal gradient have been predicted (Dalrymple and Choi, 2007) and have been reported in other rivers (Chen *et al.*, 2005; Phillips and Slattery, 2007), but previous studies have not been able to attribute these patterns to specific hydrologic variables (e.g. variation in R_h, U, Q over a tidal cycle). Our method of field measurements and calculations provided a way to examine the interaction of factors influencing energy dissipation in more detail than has previously been presented in tidal rivers.

A challenge in this study was accurately measuring water surface slope (the first term of Equation 3). The disparity between S, Q, and the consequent stream power downstream suggests that we measured water surface slope over too long a reach, resulting in periods when surface slope opposed the direction of flow velocity. Future attempts to measure surface slope along relatively short (< 10 km) reaches will require extremely precise elevation benchmarks to allow calculation of the vanishingly small water surface gradients during the transition between flood and ebb tide. Until further measurements are made, we are cautious to make conclusions regarding the similarity between measured and predicted energy dissipation in the downstream reach. Additional increase in accuracy could be achieved by direct measurement of energy slope along the non-tidal portion of the stream, alleviating the uncertainty involved with using Manning's n.

Based on these data, we suggest two hypotheses regarding the influence of tides on river morphology. First, the reduction in S at the upstream limit of tides is greater than the increase in Q, resulting in lower energy dissipation, reduced sediment transport capacity, and a tendency for channel bed aggradation and resultant channel width expansion. Second, we hypothesize that an equilibrium is reached between increasing S and Q whereby channel morphology constrains energy dissipation to levels similar to those existing before tidal influence; this expectation is based on the feedbacks between channel cross-section, shear stress, and sediment transport discussed by Friedrichs (1995). Further development and application of the technique presented here will advance efforts to predict how rivers respond to sea level rise, and help reconcile conceptual models of coastal evolution (e.g. Brinson *et al.*, 1995) with morphodynamic interpretations of stratigraphic data (e.g. Blum and Törnqvist, 2000; Dalrymple and Choi, 2007).

Acknowledgments—Nicholas Politte, Kaylyn Siporin, Ashley Smyth, Laura Stephenson, and Suzanne Thompson assisted with fieldwork. Herman Godwin and David Wilke provided access to field sites on their property. Funding was provided by the EPA STAR Graduate Fellowship #FP-91686901-0 (S.H.E.), Water Resources Research Institute of the University of North Carolina (Project #70223), NSF Career Award #0441504 (M.W.D.), and NSF EAR-0815627 (M.F.P.). The research described in this paper has been funded in part by the United States Environmental Protection Agency (EPA) under the Science to Achieve Results Graduate Fellowship Program. EPA has not officially endorsed this publication and the views expressed herein may not reflect the views of the EPA.

References

Blum MD, Törnqvist TE. 2000. Fluvial responses to climate and sea-level change: a review and look forward. *Sedimentology* **47**: 2–48.

Brinson MM, Christian RR, Blum LK. 1995. Multiple states in the sea-level induced transition from terrestrial forest to estuary. *Estuaries* **18**: 648–659.

Buschman FA, Hoitink AJF, van der Vegt M, Hoekstra P. 2009. Subtidal water level variation controlled by river flow and tides. *Water Resources Research* **45**: W10420.

Chen MS, Wartel S, Van Eck B, Van Maldegem D. 2005. Suspended matter in the Scheldt estuary. *Hydrobiologia* **540**: 79–104.

Dalrymple RW, Choi K. 2007. Morphologic and facies trends through the fluvial-marine transition in tide-dominated depositional systems: a schematic framework for environmental and sequence-stratigraphic interpretation. *Earth-Science Reviews* **81**: 135–174.

Davies G, Woodroffe CD. 2010. Tidal estuary width convergence: theory and form in north Australian estuaries. *Earth Surface Processes and Landforms* **35**: 737–749.

Ensign SH, Noe GB, Hupp CR, Fagherazzi S. 2012. A meeting of the waters: interdisciplinary challenges and opportunities in tidal rivers. *Eos* **93**: 455–456.

Friedrichs CT. 1995. Stability shear stress and equilibrium cross-sectional geometry of sheltered tidal channels. *Journal of Coastal Research* **11**: 1062–1074.

Gardner LR, Bohn M. 1980. Geomorphic and hydraulic evolution of tidal creeks on a subsiding beach ridge plain, North Inlet, S.C. *Marine Geology* **34**: M91–M97.

Knight DW. 1981. Some field measurements concerned with the behaviour of resistance coefficients in a tidal channel. *Estuarine, Coastal and Shelf Science* **12**: 303–322.

Langbein WB. 1963. The hydraulic geometry of a shallow estuary. *Bulletin of the International Association of Scientific Hydrology* **8**: 84–94.

Mohammad MB. 1961. Larval Distribution of Three Species of Balanomorpha in Relation to some Chemico-physical Factors. PhD Thesis, Duke University, Durham, NC.

Molnár P, Ramírez JA. 1998. An analysis of energy expenditure in Goodwin Creek. *Water Resources Research* **34**: 1819–1829.

Phillips JD, Slattery MC. 2007. Downstream trends in discharge, slope, and stream power in a lower coastal plain river. *Journal of Hydrology* **334**: 290–303.

Pizzuto JE, Rogers EW. 1992. The Holocene history and stratigraphy of palustrine and estuarine wetland deposits of central Delaware. *Journal of Coastal Research* **8**: 854–867.

Rhoads BL. 1987. Stream power terminology. *The Professional Geographer* **39**: 189–195.

Riley SJ. 1972. A comparison of morphometric measures of bank full. *Journal of Hydrology* **17**: 23–31.

Simpson MR, Bland R. 2000. Methods for accurate estimation of net discharge in a tidal channel. *IEEE Journal of Oceanic Engineering* **25**: 437–445.

Sweet WV, Geratz JW. 2003. Bankfull hydraulic geometry relationships and recurrence intervals for North Carolina's coastal plain. *Journal of the American Water Resources Association* **39**: 861–871.

van der Wegen M, Wang ZB, Savenije HHG, Roelvink JA. 2008. Long-term morphodynamic evolution and energy dissipation in a coastal plain, tidal embayment. *Journal of Geophysical Research* **113**: F03001.

Wright LD, Coleman JM, Thom BG. 1973. Processes of channel development in a high-tide-range environment: Cambridge Gulf-Ord River Delta, western Australia. *Journal of Geology* **81**: 15–41.

Woodroffe CD, Chappell J, Thom BG, Wallensky E. 1989. Depositional model of a macrotidal estuary and floodplain, South Alligator River, northern Australia. *Sedimentology* **36**: 737–756.